CODED EXCITATION METHODS FOR ULTRASOUND HARMONIC IMAGING

Roozbeh Arshadi, Alfred C.H. Yu, and Richard S.C. Cobbold
Institute of Biomaterials and Biomedical Engineering, University of Toronto
163 College Street, Toronto, ON, Canada. M5S 3G9
cobbold@ecf.utoronto.ca

ABSTRACT

Coded excitation methods offer the potential for improving the SNR without increasing the peak transmitted power and without sacrificing resolution. Our study examines the potential application of coded waveforms, specifically FM chirps, in harmonic imaging. Such a system, in which nonlinear echoes from tissue are used to form the image, requires the extraction and compression of the second harmonic portion of the echo signal. Our objective is to obtain the second harmonic using just one transmission, thereby avoiding problems of frame rate reduction and movement artifacts associated with multiple transmission schemes. With the help of an efficient method for predicting the transient nonlinear field from a focused transducer, design issues such as waveform and bandwidth selection, as well as filters for second harmonic extraction and compression are examined. Simulations reveal the presence of axial sidelobes in the compressed echo waveform as the bandwidth of the transmitted chirp is increased. These sidelobes, resulting from the overlap of the fundamental and third harmonic bands with the second harmonic, cannot be removed using conventional Fourier filtering. Alternative filtering techniques which utilize the separation of the harmonic bands of a backscattered chirp in the joint time-frequency domain are suggested.

SOMMAIRE

Les méthodes d'excitation codée ont le potentiel d'améliorer le ratio signal-bruit sans augmenter la puissance maximale transmise et sans sacrifier la résolution. Notre étude examine l'application potentielle de formes d'onde codées, plus spécifiquement de compression d'impulsions FM pour imagerie harmonique. Dans un tel système, les échos non-linéaires provenant du tissu sont utilisés afin de former l'image, ce qui requiert l'extraction et la compression de la deuxième portion harmonique du signal d'écho. Notre objectif est d'obtenir le deuxième harmonique en utilisant seulement une transmission, évitant ainsi des problèmes de réduction du temps d'image et d'artefacts de mouvement associés avec de multiples schémas de transmission. En utilisant une méthode efficace de prédiction du champs non-linéaire transitoire provenant d'un transducteur focalisé, des problèmes de conception tels que la sélection de forme d'onde et de la largeur de bande, ainsi que de filtres pour l'extraction et la compression du deuxième harmonique sont examinés. Les simulations révèlent la présence de lobes latéraux axiaux dans la forme d'onde compressée au fur et a mesure que la largeur de bande de la compression d'impulsion transmise est augmentée. Ces lobes latéraux, dus au chevauchement de la bande harmonique fondamentale et de la troisième bande avec la deuxième bande harmonique ne peuvent pas être enlevés en utilisant le filtrage conventionnel de Fourier. En tant qu'alternative, des techniques de filtrage utilisant la séparation de bandes harmoniques de compressions d'impulsions rétrodiffusés dans le domaine commun de temps-fréquence sont suggérées.

1. INTRODUCTION

Coded excitation methods have been used in ultrasound imaging to improve the signal-to-noise ratio (SNR) and to maintain a high axial resolution at greater distances without increasing the peak transmitted power. As recently reviewed by Cobbold (see Sec. 8.4 in [1]), these methods were initially developed in the radar research field in the 1950s. Their application to medical ultrasound started in the 1970s when they were first used to improve the performance of flow estimation [2] and tissue imaging [3][4]. In terms of their performance in ultrasound systems, coded excitation methods can achieve SNR gains in the range of 15-20 dB [5]. This improvement is comparatively more modest than the ones achievable in radar systems, where SNR gains on the order of several thousands are often possible.

The development of coded excitation schemes was originally motivated by Woodward's theoretical studies on the range ambiguity problem in radar systems [6]. In particular, it was postulated that a long-duration transmit

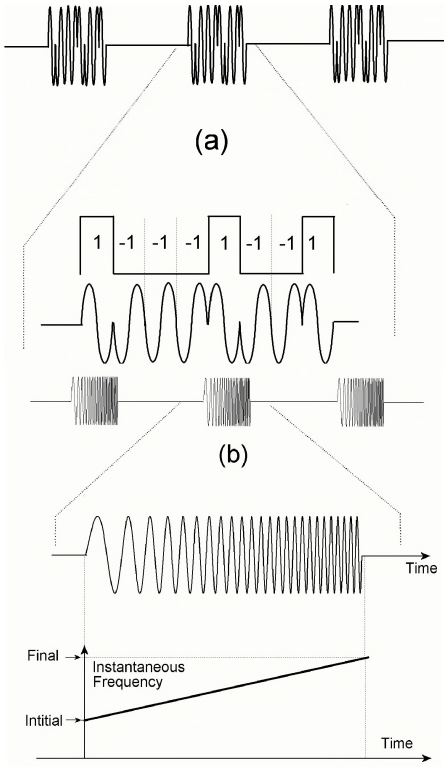

Figure 1. Types of coded excitation schemes applicable to ultrasound imaging. (a) Binary encoding (a single-cycle sinusoidal transmitted pulse has been assumed). (b) Linear frequency-modulated (FM) chirp.

waveform could be used to increase the total transmitted energy while maintaining the same peak power without any loss in spatial resolution. Even though coded signals are generally longer duration than non-coded ones, the potential loss in spatial resolution can be avoided by using a compression filter that matches the pulse echoes with the transmitted signal's time-reversed conjugate. Note that the resulting signal obtained from the cross-correlator is often known as the compressed waveform.

In the radar literature, a number of schemes have been proposed for coded excitation (see Ch. 6 & 8 in [7]). However, the applicability of many of these coding schemes in medical ultrasound is limited by the effects caused by the high attenuation of tissue and tissue motion. Nevertheless, two particular coding schemes – namely, binary codes and frequency-modulated (FM) chirps (see Figure 1) – are important for achieving significant SNR improvements in ultrasound [8]. In their comparison of these two schemes, Misaridis and Jensen [9][10] argued that binary codes appear to be suboptimal because the sharp transitions in between binary states are very high frequency contents that tend to be truncated by the limited transducer bandwidth and the effects of frequency-dependent attenuation in tissues. Based on this argument, it seems to be more appropriate to focus on the FM-chirp coding method.

Although the use of coded excitation in ultrasound imaging is well established, there have been few studies that considered the potential use of these methods in tissue harmonic imaging where the nonlinear ultrasound echoes returned from tissues are used to form images. As such, the purpose of this paper is to use simulation means to examine the primary issues related to the use of linear FM chirps for improving the SNR performance in tissue harmonic imaging. The simulations are based on the use of FM chirp coding in a single-firing harmonic imaging scheme, and these results are compared with the ones obtained from a two-pulse harmonic imaging scheme known as pulse inversion [11]. To facilitate presentation of the simulations, we shall start with brief reviews of FM chirp coding and harmonic imaging methods. Details of the simulations scheme used in our studies will subsequently be described.

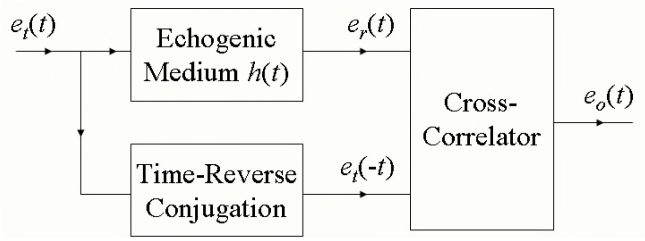

Figure 2. Generic diagram for a compression filter in which the output is the cross-correlation of the received signals and the transmitted pulse's time-reversed conjugate.

2. THEORY

2.1. Principles of FM Chirp Methods

Background Considerations

Consider the pulse compression filter shown in Figure 2, where the pulse-echo impulse response of a given echogenic medium is denoted by $h(t)$. If the transducer is excited by a waveform $e_t(t)$ and if the filtering effect of the transducer is ignored, then the received waveform $e_r(t)$ is given by the following convolution:

$$e_r(t) = e_t(t) * h(t) = \int_{-\infty}^{\infty} e_t(t-\tau)h(\tau)\,d\tau \,. \tag{1}$$

Also, the compressed waveform $e_o(t)$ (i.e. the output of the cross-correlator) can be shown to be equal to:

$$\begin{aligned} e_o(t) &= \int_{-\infty}^{\infty} e_r(t+u)e_t(-u)\,du \\ &= \int_{-\infty}^{\infty}\left[\int_{-\infty}^{\infty} e_t(t+u-\tau)e_t(-u)\,du\right]h(\tau)\,d\tau \\ &= R_{ee}(t) * h(t) \end{aligned} \tag{2}$$

where $R_{ee}(t)$ is the autocorrelation of $e_t(t)$. From (2), it can be seen that the compressed waveform is the convolution between the transmitted signal's autocorrelation function and the medium's impulse response.

General Principles

In general, a unit-amplitude FM chirp pulse whose instantaneous frequency varies linearly with time can be expressed as:

$$e_t(t) = \mathrm{rect}(t/T)\cos\left(\frac{kt^2}{2} + \omega_o t\right) \quad \text{for } |t| < \frac{T}{2}, \tag{3}$$

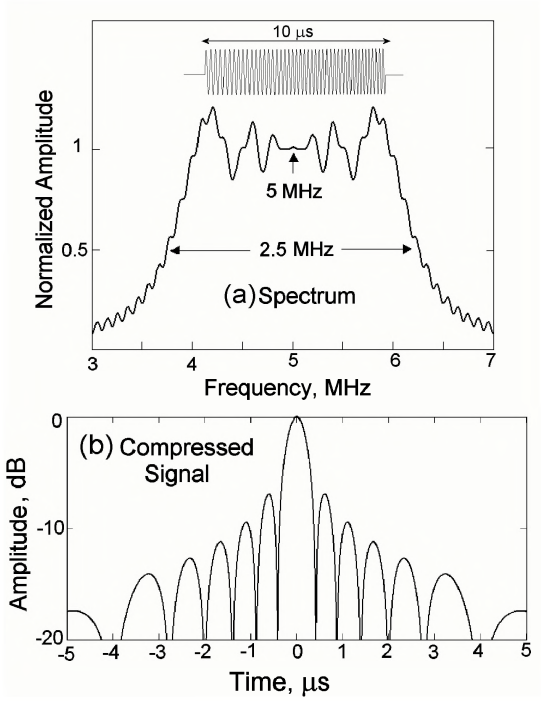

Figure 3. A non-tapered linear FM chirp of 10 μs duration, 5MHz center frequency, and 2.5MHz signal bandwidth. (a) Frequency spectrum as calculated from (4). (b) Envelope of the compressed signal as calculated from (3) without the cosine term (the total compressed signal duration is 20 μs).

where T is the pulse duration, ω_o is the center angular frequency, and k is a chirp rate parameter that controls the pulse bandwidth. Note that the instantaneous frequency of (3) is given by $\omega(t) = d\varphi/dt = \omega_o + kt$, where φ is the argument of the cosine function.

To illustrate the use of FM chirps in a coded excitation system, we consider a basic imaging scenario where the echogenic medium only contains a single point target. For such a scenario, the medium's response is simply equal to an impulse $[h(t)=\delta(t)]$, and correspondingly the compressed waveform defined in (2) is simply equal to the transmitted signal's autocorrelation function. Hence, if the FM chirp of (3) is fired into this single-target medium and if the filtering effect of the transducer is ignored, the resulting compressed waveform at the receiver output can be shown to be given by (see Sec. 6.2 in [7]):

$$e_o(t) = \sqrt{\frac{2k}{\pi}}\,\mathrm{rect}\left(t/2T\right)\frac{\sin\left[kt(T-|t|)/2\right]}{kt}\cos(\omega_o t)\cdot \qquad (4)$$

From the rect() term in the above expression, it can be seen that the compressed waveform actually extends over twice the initial chirp duration, i.e., from $-T$ to $+T$. Also, its envelope generally follows a pseudo-sinc shape as described by the $\sin[kt(T-|t|)/2]/kt$ term. Aside from the time-domain expression, it is also worth considering the compressed waveform's spectrum (which is simply the FM chirp's spectrum in this case). From Fourier analysis, this spectrum can be shown to be given by (see Sec. 6.3 in [7]):

$$E_o(\omega) = \sqrt{\frac{\pi}{4k}}e^{-j(\omega-\omega_o)^2/2k}\left[F^*(X_1)+F^*(X_2)\right], \qquad (5)$$

where $X_1 = [kT/2+(\omega-\omega_o)]/(k\pi)^{1/2}$, $X_2 = [kT/2-(\omega-\omega_o)]/(k\pi)^{1/2}$, and $F^*(X)$ is the complex conjugate of a Fresnel integral.

The above expressions can be illustrated through the example shown in Figure 3, where a 10 μs FM chirp with a center frequency of 5 MHz and a bandwidth of 2.5 MHz is assumed. Note that such a waveform has time-bandwidth product that is 25 times larger than a non-chirped pulse echo scheme. As can be seen from the figures, the compressed waveform contains *range sidelobes* (sometimes referred to as *self-noise*) with amplitudes comparable to the main lobe. As discussed by Kowatsch and Stocker [12], the sidelobes are a result of the rect() time window inherent in the transmitted chirp pulse and are directly related to the Fresnel ripples seen in the frequency spectrum. In the presence of multiple scattering targets, these sidelobes will lead to difficulties in detecting a weakly scattering target because its main lobe may be masked out by the range sidelobes of a strongly scattering target located nearby.

Pulse Shaping Considerations

To account for the sidelobe problem when using FM chirps, much effort has been devoted towards devising schemes for reducing the range sidelobe level to well below –50 dB. For instance, time-domain shaping of the transmit pulse can be used to smooth out the sharp edges associated with the chirp pulse's rectangular window. One useful way

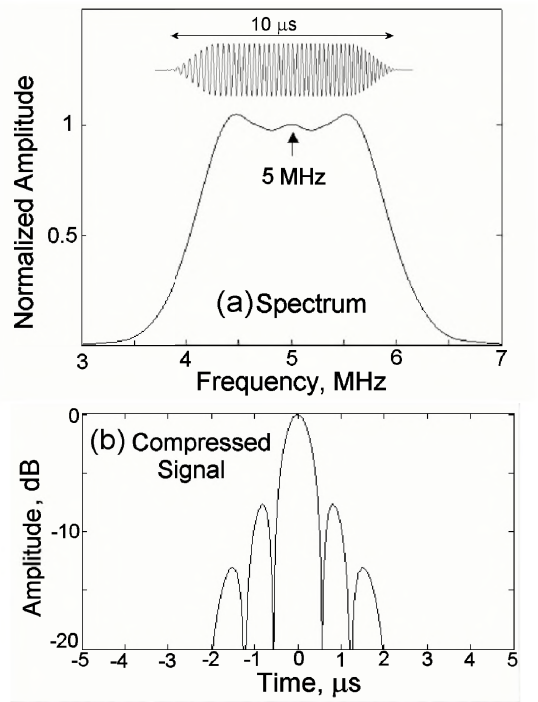

Figure 4. Effect of cosine (Tukey) amplitude tapering on the compressed envelope. Other signal parameters are the same as those in Figure 3. (a) Transmitted waveform with a cosine taper over the first and last 2.25 μs and its spectrum. (b) Envelope of the compressed signal.

of shaping a chirp pulse is to apply a cosine taper (i.e., a Tukey window) to the leading and trailing parts of the waveform. As can be seen in Figure 4, the tapered chirp

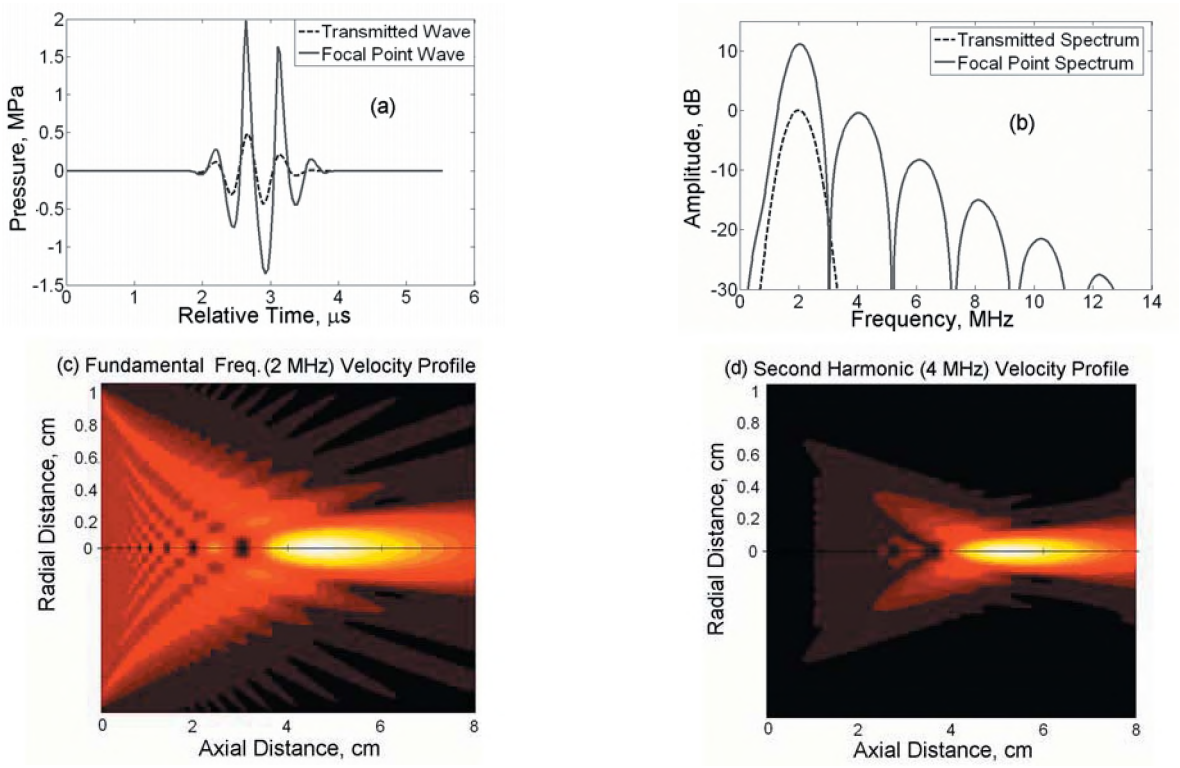

Figure 5. Simulated waveforms and profiles from transmission of a Gaussian pulse of p_o=500 kPa, f_c=2 MHz, and 60% -6 dB fractional bandwidth, from a 1 cm radius focused transducer (F= 6 cm) into a tissue-like medium (α_0 = 0.04 Np/cm/MHz, β = 4.75, c_o=1546 m/s). (a) Comparison of the transmitted waveform to the waveform at the focal point, demonstrating distortion due to nonlinearity. (b) Comparison of the spectrum of the transmitted waveform to the waveform at the focal point, demonstrating generation of new harmonic bands. (c) Normal velocity profile of the 2 MHz component of the waveform as it propagates into the medium, note the presence of lateral sidelobes. (d) Normal velocity profile of the 4 MHz component of the waveform as it propagates into the medium. Note that the lateral sidelobes do not extend very far in the lateral direction.

pulse has a much smoother spectrum, which in turn leads to significant reduction in the range sidelobes. It is worth noting that the bandpass nature of the transducer's transfer function may also be exploited to achieve similar spectral smoothing effects. In particular, if the transducer bandwidth is narrower than that of a non-tapered chirp pulse, then it is equivalent to applying a frequency-domain window to the chirp pulse's spectrum. This effect has been examined in a few studies [10][13], which showed that the transfer function of the transducer can cause a substantial reduction in the range sidelobes. Despite their advantages, however, it is important to note out that pulse shaping and spectral smoothing would concomitantly lead to a SNR reduction of a few dB and a slight loss of axial resolution due to broadening of the main lobe.

2.2. Principles of Harmonic Imaging

Background Considerations

As reviewed by Cobbold (see Sec. 8.6 in [1]), there are generally two approaches to harmonic imaging: one based on the use of a contrast agent like microbubble, and the other based on the generation of nonlinear waves in tissue. The basic rationale behind the first approach is that the nonlinear scattering properties of ultrasound contrast agents can generate signal harmonics in regions where the agents are located and in turn enhance the local signal contrast. As such, the imaging process associated with the use of contrast agents is often called *contrast media harmonic imaging*. On the other hand, the main principle behind the second approach is that tissue can too become a nonlinear scattering medium if the incident pressure fields are sufficiently high and thereby give rise to harmonic echoes. This second form of imaging, generally called *tissue harmonic imaging*, is the subject of discussion in this paper.

General Principles

To illustrate the field excitation principles behind tissue harmonic imaging, Figure 5 shows the fundamental and second-harmonic field profiles produced by transmitting a wideband Gaussian pulse from a focused disc transducer into a tissue-like medium. As seen in part (a) of this figure, there is substantial distortion (in the form of spiky wave peaks) in the incident waveform at the focal point. It turns out that these distortions are due to the signal harmonics being generated in the focal region (see (d) of the figure). On a different note, it is worth pointing out that the second-harmonic field profile is significantly more focused than its fundamental counterpart. Such focusing improvement is well-recognized as the theoretical advantage of producing images from harmonic echoes. However, a major limitation

of using harmonic echoes for imaging is that their signal strength is at least 10 dB weaker than the fundamental signals (see part (b) of figure). To address this limitation, it is beneficial to develop a technique that can boost the SNR in harmonic imaging (especially when examining for deeper structures). As suggested in some studies [10][14][15][16], the use of coded excitation may be a potential solution for such SNR improvement needs. This technique is the focus of our simulation study, and it will simply be referred to as *coded harmonic imaging* from hereon.

2.3. Design Considerations in Coded Harmonic Imaging

Pulse Selection Issues

As pointed out by Misaridis and Jensen [10], FM chirps maintain their coded phase relationship in the harmonic domain – i.e. the higher harmonics are also chirps and can be compressed using appropriately matched filters. Hence, when using FM chirps for coded harmonic imaging, compression filters like the ones for chirp-based coded excitation can be used to obtain the compressed harmonic waveform. In view of this advantage, FM chirps appear to be logical candidates for use in coded harmonic imaging. On the other hand, the use of binary codes in harmonic imaging appears to be more challenging because the phase coding relationship for fundamental signals does not carry over for harmonic echoes. This type of code is not considered in this paper. Nevertheless, it is worth noting that there are some special forms of binary codes that may be potentially useful for coded harmonic imaging [14].

Bandwidth Issues

The transmitted signal bandwidth is an important parameter in ultrasound B-mode imaging since bandwidth directly affects the axial resolution. The impact of this signal parameter in conventional harmonic imaging is also well-known: if the transmitted signal is wideband, then adjacent harmonics in the received signal may overlap in frequency. The potential occurrence of this spectral leakage creates a problem since it makes difficult for a conventional highpass filter to distinguish the spectral harmonics from the fundamental. In particular, with spectral leakage, the highpass filter can suppress the leaking fundamental signal only if some of the desired harmonic echoes are removed concomitantly, or else some of the fundamental signal will still remain. A well-known solution to such problem is to use a two-pulse transmission scheme known as "pulse inversion" (which transmits a pulse and its negated form in sequence) and then sum the two complementary pulse echoes to cancel out the fundamental signal while retaining the harmonic echoes. Nevertheless, because two firings are needed, this approach inherently leads to a reduction in frame rate. As well, as examined by Shen and Li [17], its efficacy is susceptible to spectral leakage problems when tissue motion is present.

In coded harmonic imaging, the problem of spectral leakages is even more significant. The reason is because the compression filtering procedure used to recover the axial resolution is often matched to the transmit pulse shape, and thus the harmonic compression performance will be reduced if there is a significant amount of spectral leakage present in the received signal. In turn, the compressed harmonic signal (usually done for the second harmonic) may suffer in the form of loss in axial resolution, contrast resolution, or SNR. The impact of spectral leakage on the compressed harmonic signal will be examined in detail in our simulations.

3. SIMULATION METHOD

3.1. General Overview

For all the simulations reported in this study, the pressure field was generated by a single focused circular transducer with a radius of 1 cm and a focal length of 6 cm. The medium was characterized by the following parameters of a tissue mimicking material similar to liver tissue: acoustic attenuation $\alpha = \alpha_o f$ (with $\alpha_o = 0.04$Np/cm/MHz), nonlinearity parameter $\beta = 4.7$, sound propagation speed $c_o = 1546$m/s, and density $\rho = 1000$kg/m^3. Ultrasound propagation in this medium was simulated by using a second-order operator splitting approach that uses a fractional step-marching scheme, whereby the effects of diffraction, attenuation, and nonlinearity can be computed independently over incremental steps [18]. To calculate the effects of diffraction, we took advantage of the cylindrical symmetry of the problem by making use of the Hankel transform [19] rather than the less efficient angular spectrum approach. The return echo from a single point scatterer is assumed to propagate linearly to the transducer, where the integrated received signal is processed by the receiver filter, which includes compression filtering for coded waveforms, and finally the display processing. Our simulation results assumed a homogenous medium and a sufficiently wideband transducer so as not to affect either the transmitted or received signals.

3.2. Transmitted Signal

In order to determine the effect of bandwidth on the desired second harmonic signal, linear FM chirps with -6dB fractional bandwidths ranging from 10-80% were simulated and the waveforms at the focal plane were recorded. In these simulations, a constant chirp duration of 20 μs and a center frequency of 2 MHz were used. Also, for comparison, the results from a conventional (non-coded) Gaussian pulse with the same fractional bandwidth and peak pressure were also simulated.

As pointed out earlier, the pulse shaping window has a significant influence on the sidelobe level and affects the mainlobe width. Hence, as part of the study, we investigated the effects of the following three pulse shaping windows:

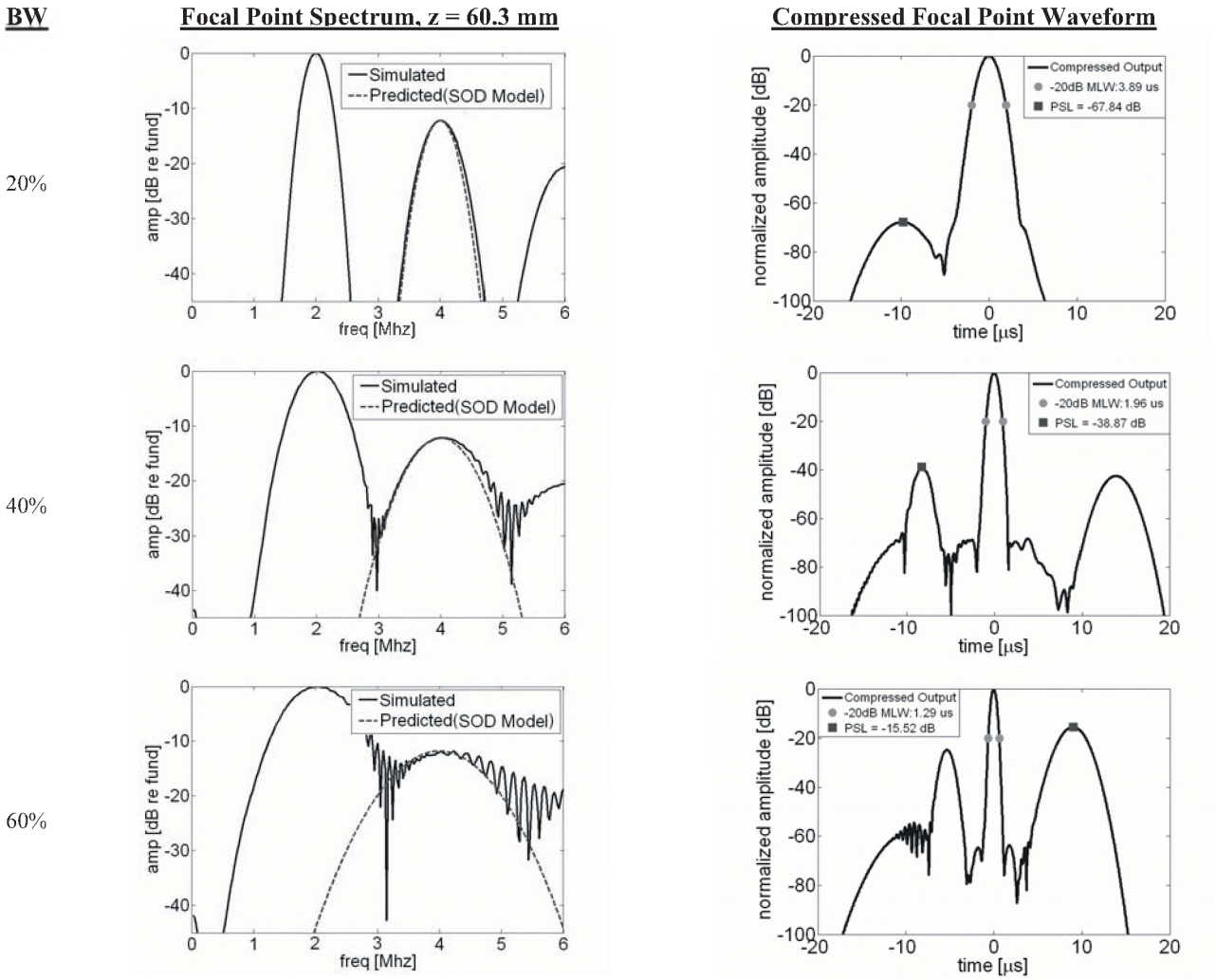

Figure 6. The left column shows the spectrum of the waveform at the focal point for transmitted chirps with fractional bandwidths of 20%, 40% and 60% and their comparison to the second harmonic as predicted by the second order distortion (SOD) model. The right column shows the corresponding compressed waveforms obtained from the SOD compression filter. The -20 dB mainlobe width and the peak side lobe levels (PSL) are marked. Note the increasing sidelobes associated with spectral leakage as the bandwidth is increased.

1. Gaussian (with $\chi = 3$, where χ is the reciprocal of the standard deviation);
2. Tapered Cosine (with R=0.65, corresponding to Matlab's *tukeywin.c*);
3. Rectangular (i.e. no tapering).

3.3. Receiver Processing

In the absence of any coding, the receiver typically includes filtering to remove components outside the second harmonic band, followed by envelope detection and display on a log scale. Another way of distinguishing the second harmonic band in non-coded imaging is to use the pulse-inversion firing scheme that involves two firings along each path (as we noted earlier). On the other hand, for FM chirps, the receiver processing must include compression filtering in order to recover the axial resolution of the received echoes. In a single firing system, the coded received signal is often passed directly to the compression filter, although bandpass filters can be used to remove some unwanted components before compression. Alternatively, if pulse inversion is used during coded harmonic data acquisition, then the field generated by both the original pulse and its negated form must first be calculated, the corresponding echoes summed together, and then passed directly to the compression filter.

3.4. Compression Filter Model

In the design of chirp-coded harmonic systems, Kim et al. [16] made use of a square law model (also known as a second order distortion model) of the propagation process to design a compression filter. Ignoring higher harmonics, this model assumes that the received signal from nonlinear propagation can be approximated as $r(t) = a_1 s(t) + a_2 s^2(t)$, where a_1 and a_2 are constants that characterize the nonlinear propagation process and $s(t)$ is the transmitted signal. This seems to be a suitable signal model since the second

harmonic is the strongest among the nonlinear harmonics; hence, it was used to predict the second harmonic portion of the received signal on which the compression filter is based. In fact, the impulse response of our compression filter for the second harmonic was defined as the time-reversed conjugate of $s^2(t)$. In the discussion given below we refer to such a compression filter as an SOD compression filter.

3.5. Performance Evaluation

For the purpose of analyzing the behavior of a coded waveform under nonlinear propagation conditions, the waveforms obtained using the aforementioned step-wise nonlinear simulator are analyzed mainly at two locations. The first is the radiation pattern at the focal plane where we can analyze the spectrum of the on-axis waveform and even apply the receiver processing directly to the waveform. The second location is at the transducer where the compressed harmonic signal can be analyzed after compression filtering.

Whether we apply the receiver processing to the focal plane signal or the received signal from a scatterer, the system performance can be quantitatively assessed by using several criteria corresponding to axial resolution, contrast resolution, and gain in SNR [9][10]. These criteria are generally used to analyze the compressed harmonic signal that is ready for display – i.e., the waveform has been processed, envelope detected and changed to a dB scale reflecting the dynamic range of the system. In our study, the -20 dB mainlobe width (MLW) of the processed time domain signal is used to assess axial resolution. The Peak Sidelobe Level (PSL) and Integrated Sidelobe Level (ISL) are also used to assess contrast resolution. In addition, the gain in SNR is assessed by finding the ratio between the peak of a compressed harmonic signal and that of a processed non-coded signal obtained from a Gaussian pulse with equal peak pressure and bandwidth.

4. RESULTS

4.1. Spectral Overlap and Effects on Compression

The left column in Figure 6 shows the spectrum of the received signal at the focal point for three transmitted Gaussian-windowed FM chirps of increasing fractional bandwidths. These focal point spectra indicate that as the bandwidth is increased, the fundamental and third harmonic bands overlap with the second harmonic band, resulting in periodic fluctuations in the spectrum as well as deviations from the assumed second order distortion model (dashed lines). Note that the nature of the overlap and its effects on spectrum shape are different than those seen with non-coded pulses. In particular, the spectral overlap is not in the form of random dephasing; instead, it is in the form of periodic fluctuations that result from the nonlinear phase of the transmitted FM chirp and its harmonics. The effects of this spectral overlap on the compressed harmonic signal can

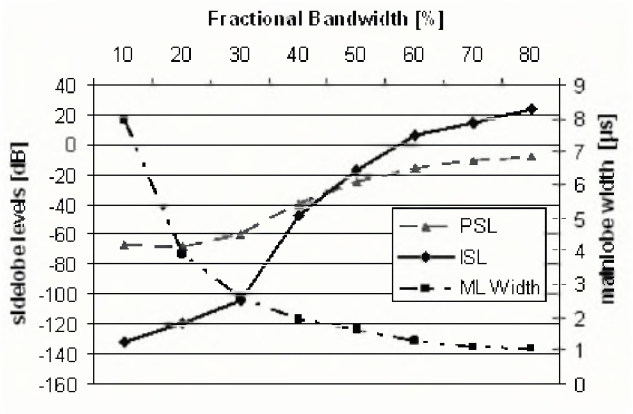

Figure 7. Effect of bandwidth on coded harmonic compression for a Gaussian transmitted signal. As fractional bandwidth of the transmitted signal is increased, the peak sidelobe level (PSL) and integrated sidelobe levels (ISL) of the compressed waveform are increased, while the mainlobe width, which is an indicator of axial resolution, is decreased.

be seen in the right column of Figure 6. As can be seen, significant sidelobe levels are produced as bandwidth is increased, even though there is improvement in the mainlobe width (and in turn the axial resolution). These sidelobes reach levels of greater than –40 dB for 40% and –20 dB for the 60% transmitted bandwidth.

For the Gaussian FM chirp, the performance criteria based on the compressed harmonic waveforms have been tabulated and are shown in Figure 7. Note that, for chirps with fractional bandwidths less than 40%, the mainlobe width appears to increase significantly and hence the axial resolution may be too low for imaging purpose. However, when the fractional bandwidth is greater than 40%, there is a substantial increase in the peak sidelobe levels (PSL) and their relative energy to the mainlobe (ISL). This pattern of increasing sidelobes at greater bandwidths also applies to the non-Gaussian chirp signals; in fact, depending on the tapering, some waveforms exhibit large sidelobes even at lower bandwidths. To suppress these high sidelobe levels, it is necessary to carry out some form of pre-processing (e.g., filtering) or use a more advanced compression filter.

4.2. Use of Pulse Inversion Prior to Compression

To confirm the role of spectral overlap in creating the high sidelobe levels, the above analysis was repeated on received signals whose fundamental and odd harmonics were suppressed with the pulse inversion method. The corresponding focal point spectra before compression are shown in Figure 8. As can be seen, the spectrum of the second harmonic in this case looks much closer to the second order distortion model since the fundamental and third harmonic bands are both suppressed via pulse inversion. Interestingly, there are still the some differences in the two spectra near 6 MHz, and these differences are likely due to the spectral overlap between the second and

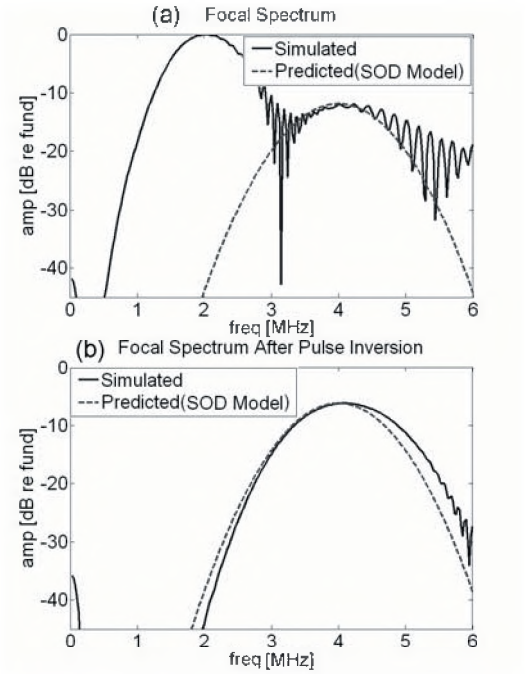

Figure 8. Effect of pulse inversion on the spectrum of the focal point waveform (bandwidth=60%). (a) Spectrum of the waveform at the focal point. (b) Spectrum obtained from addition of the focal waveform from transmission of a positive LFM and that from transmission of the inverted LFM waveform. The SOD model also plotted for reference.

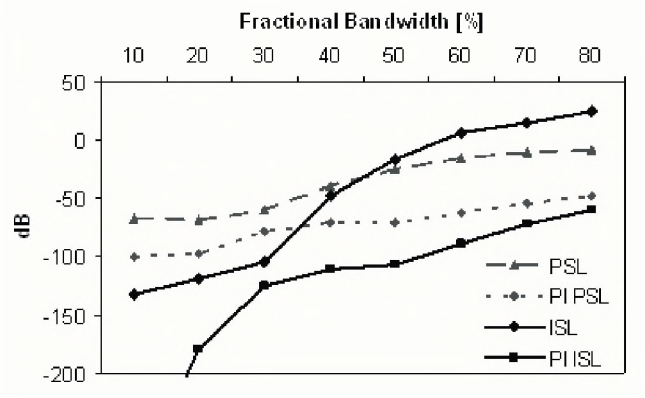

Figure 9. Effect of bandwidth on coded harmonic compression when using pulse inversion (PI). PSL–peak sidelobe level; ISL–integrated sidelobe level.

fourth harmonics. As will be shown shortly though, they do not appear to have much impact on the compression results.

As seen in Figure 9, the effect of pulse inversion (i.e., spectral overlap reduction) on the compression performance is evident by noting the reduced sidelobe levels in the compressed harmonic waveform. In particular, for fractional bandwidths greater than 40%, PSL levels have decreased by 30-40 dB while the ISL levels have reduced by as much as 80 dB. Nevertheless, it is important to bear in mind that such performance improvements come at a cost of reduced frame rate (two firings are required) and potential spectral leakage due to tissue motion [17].

4.3. Use of Conventional Filtering Prior to Compression

Perhaps a straightforward way of suppressing the sidelobes in the compressed harmonic signal is to use bandpass filtering before compression to retain only the second harmonic components. However, in doing so, we are faced with the same problem which plagues the single-firing harmonic imaging approach – that is, the desired harmonic band and the leaking bands are not completely separable in the frequency domain. In fact, this problem is more severe in the case of coded harmonic imaging due to compression filtering.

To demonstrate the pitfalls of conventional bandpass filtering, the focal-point received signal corresponding to a 60%-bandwidth chirp excitation was filtered using several ideal bandpass filters prior to compression. Figure 10a shows two examples of such bandpass filters on top of the received spectrum. The 3.25-5.25 MHz filter has reduced one of the compression sidelobes significantly – as seen in Figure 10b – yet the sidelobe levels are still within the 45 dB dynamic range. If we narrow the bandpass filter to 3.5-5.0 MHz, the secondary sidelobes are reduced further, but the mainlobe starts to widen along with its own increasing sidelobes. This inherent tradeoff between sidelobe level and mainlobe width is indeed the primary limitation of using conventional bandpass filtering to reduce the sidelobes in the compressed harmonic signal.

A potential alternative approach is to make use of second order Volterra filters. This method was examined and applied by Phukpattaranont and Ebbini [20] for separating the quadratic component generated by contrast agents for use in imaging.

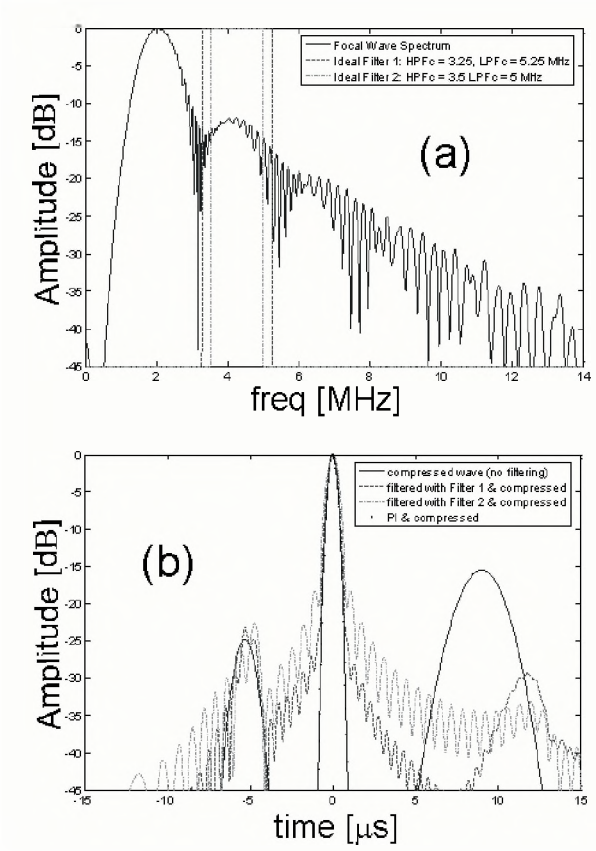

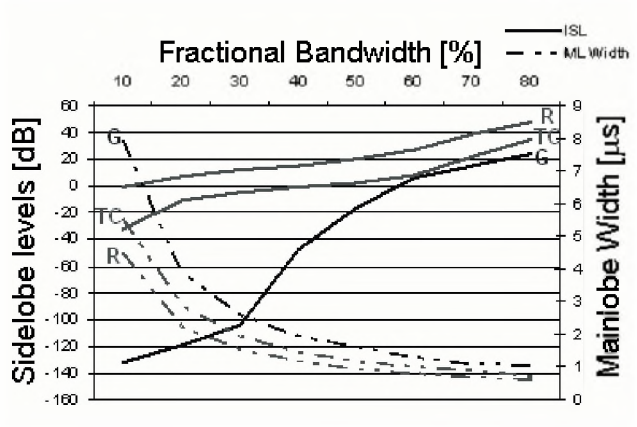

Figure 11. Effect of waveform tapering and bandwidth on coded harmonic compression. The graph compares the integrated sidelobe levels (ISL) and mainlobe width after compression for three types of pulse shaping: Rectangular (R), Tapered Cosine (TC), and Gaussian tapering (G).

4.4. Pulse Shaping and Effects on Compression Results

In the previous few sections, the presented results were obtained using Gaussian-windowed FM chirps. To generalize these findings, the analysis was repeated using other types of pulse shaping windows. The corresponding results are summarized in Figure 11, which shows a comparison on the mainlobe width and sidelobe levels of the compressed harmonic waveform obtained from transmission of three different types of tapered FM chirps. As can be seen, if a rectangular window (i.e., no tapering) is used on the transmitted signal, then high-energy sidelobes are present in the compressed harmonic signal even at small bandwidths. As transmitted signal tapering increases (from none to tapered cosine to Gaussian), these sidelobes become less prominent. On the other hand, an opposite trend is observed for the mainlobe width: no tapering actually gives narrower mainlobe widths and hence yields better axial resolution. After all, the choice of tapering is influenced by tradeoff issues between axial resolution (sidelobe levels) and temporal resolution (mainlobe width). Note that, in a practical situation, the finite operating bandwidth of the transducer would further complicate the choice.

Even though we have chosen to apply the tapering directly to the transmitted waveform, it is not the only way to reduce sidelobe levels. Alternatively, the tapering can be applied to the compression filter's impulse response so that as much energy as possible can be physically transmitted. As studied carefully by Misaridis and Jensen [9][10], such a filter can be considered as a mismatched filter.

4.5. Gain in SNR Due to Coding and Compression

As discussed previously, the purpose of coding is to increase the signal to noise ratio without changing the peak transmitted power and thereby improving the penetration range. To demonstrate this theoretical advantage, Figure 12 shows the gain in SNR by comparing the result from transmission of a non-coded pulse to that of a 20 μs coded FM chirp of equal fractional bandwidth (60%). Note that, for the non-coded pulse, pulse inversion was used to extract the second harmonic while suppressing the odd harmonics. As for the FM chirp, a compression filter based on the second order distortion model was applied to the received waveforms to obtain the compressed harmonic signal, and the procedure was repeated for received signal obtained with pulse inversion.

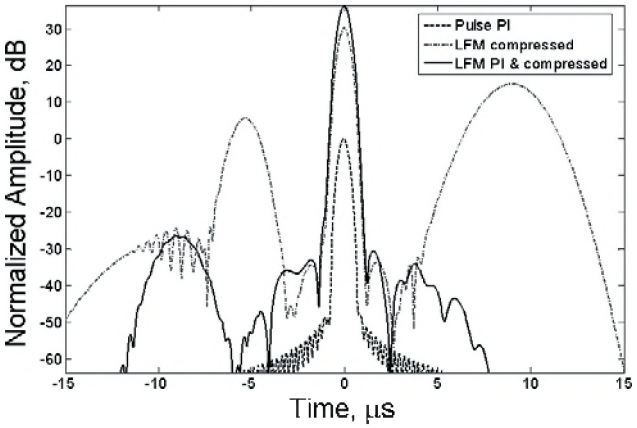

Figure 12. Gain in SNR as a result of coding. Even though axial sidelobes are present, compression has recovered the axial resolution and increased the SNR. Note the peak of the mainlobe of the compressed LFM is more than 30 dB greater than the non-coded pulse peak.

By comparing the mainlobe peaks from Figure 12, it can be seen that the FM chirp's compressed harmonic signal has an SNR gain of approximately 30 dB as compared to the non-coded pulse's received signal. Additionally, the figure confirms the benefits of suppressing the spectral overlap in the received spectra prior to compression filtering, even though the suppression was achieved using pulse inversion. Another observation evident in this figure is that the compressed harmonic signal of the FM chirp actually has a mainlobe width approximately the same as that of the non-coded pulse. This result demonstrates the ability of chirp-based coded excitation methods in obtaining compressed harmonic waveforms with high axial resolutions.

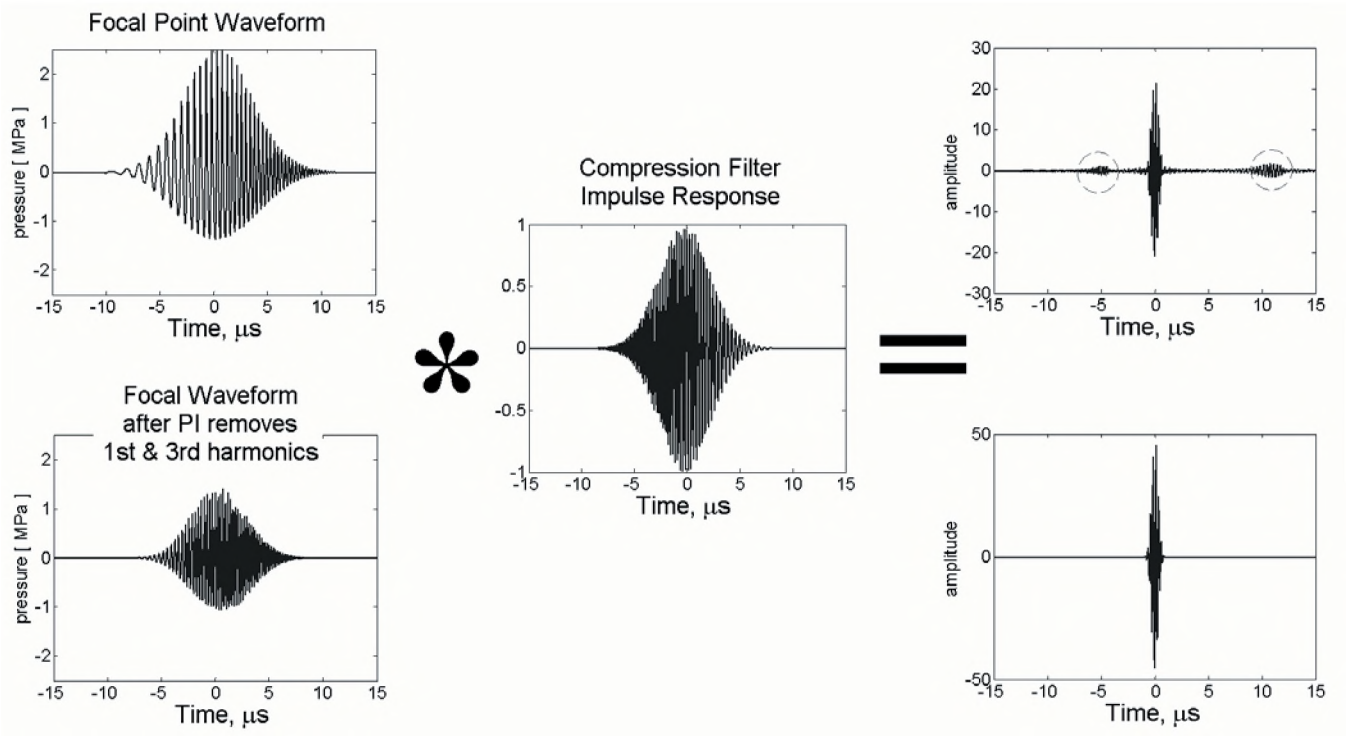

Figure 13. Example of a focal point waveform (a harmonic chirp signal) and the resulting waveform after convolution with the impulse response of the compression filter. The smaller circled waveforms to the right and left of the compressed waveform are due to the leaking fundamental and third harmonic portions of the chirp. Note that they disappear (lower part) after the fundamental and third harmonic portions of the focal waveform have been removed using the pulse inversion technique.

4.6. Compression Filtering Issues

The simulation results presented throughout this section have shown that, as the bandwidth of the transmitted FM chirp is increased to improve resolution, the spectral leakage between harmonics would give rise to high sidelobe levels in the compressed harmonic signal. In this section, we shall further discuss the origin and nature of these sidelobes and examine the potential of removing them without the need for pulse inversion by taking advantage of a chirp's time-frequency domain properties.

We begin by recalling that, as the transmitted FM chirp propagates into the medium, the waveform gradually gets distorted as the focus is approached, thereby leading to the generation of new harmonic frequencies. Nevertheless, the harmonics would still retain their coded properties (i.e., the nonlinear phase relationship which defines a chirp). Hence, the return echo at a specific point may be approximated by a higher-order signal model $r(t) = a_1 s(t) + a_2 s^2(t) + a_3 s^3(t) + \ldots$. The upper-left plot of Figure 13 shows a single-point pulse echo simulated using a third-order signal approximation and a 20 μs Gaussian FM chirp with 60% bandwidth. To process this coded received signal, it should be noted that a compression filter matched to $s^2(t)$ is the most reasonable choice because the exact parameters of the medium (i.e. nonlinearity, attenuation, etc.) are unknown in practical situations. In Figure 13, such a compression filter is used to compress the focal waveform, and the results are shown in the upper-right plot. Note that, in addition to the desired compressed second harmonic (i.e. the mainlobe), two smaller waveforms are present at its left and right (i.e. the sidelobes). On a dB scale, the magnitudes of these smaller waveforms are actually comparable to the main compressed waveform. In contrast, when pulse inversion is used to remove the fundamental and the third harmonic in the simulated waveform (bottom-left plot of Figure 13), the undesired sidelobes would disappear from the compressed harmonic signal (bottom-right plot). This result confirms that the sidelobes are caused by the leaking fundamental and third harmonic bands.

To remove the leaking bands in a single-firing system, we may be able to take advantage of properties of chirps in the time-frequency space. For instance, Figure 14 shows a typical received harmonic chirp and its corresponding waveform after compression in time, frequency, and time-frequency domains. As can be seen, the harmonics of the received chirp (left column of Figure 14) are completely overlapping in the time domain; there is also significant overlap between the harmonic bands in the frequency domain. However, in the time-frequency space of the spectrogram, the different harmonic chirps of the signal are clearly separable and have distinct time-frequency slopes. Although this example is merely based on the assumption that scatterers are well separated in space, it nevertheless illustrated the time-frequency variation characteristics of chirp echoes. In practice, it would be worthwhile to examine in more detail the time-frequency properties of

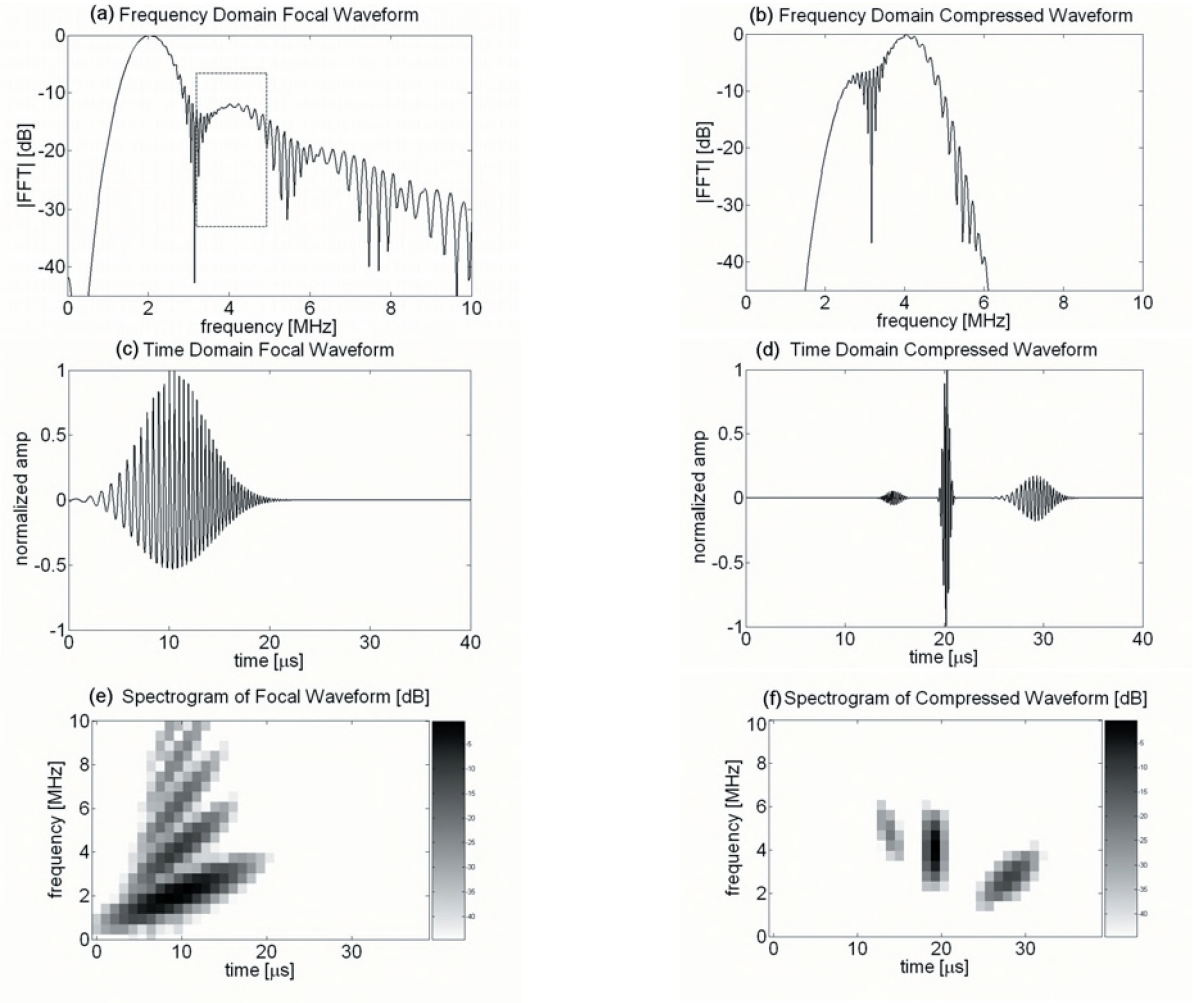

Figure 14. Typical harmonic chirp before and after compression, shown in the time, frequency, and time-frequency domains. Left column shows a typical harmonic chirp signal at the focus of the transducer; in the spectrogram, the different harmonic components of the chirp are clearly distinguishable. Right column shows the compressed waveform using a second order compression filter. While the second harmonic chirp is compressed, the leaking fundamental and third harmonic chirps result in presence of uncompressed chirps to its left and right.

chirp echoes returned from multiple scatterers that collectively give rise to signal speckling features.

More insights on the time-frequency nature of coded harmonic echoes can actually be drawn by examining the properties of the compression filter which is based on a second order distortion model. Such a filter tends to cancel out the coded phases in the second harmonic component of the received signal, thereby compressing this harmonic in the time domain as seen in the right hand column of Figure 14 (here again, the assumption of well-separated scatterers should be noted). In the time-frequency domain, the compressed second harmonic would correspond to a component with infinite time-frequency slope (i.e. parallel to the frequency axis). On the other hand, the spectral leakage components originating from the fundamental and the third harmonic would emerge in the spectrogram as chirps to the left and right of the desired second harmonic. In fact, as evident in Figure 14, leakages from the fundamental would give rise to a longer chirp to the right of the compressed second harmonic, while leakages from the third harmonic would give rise to the smaller and shorter chirp to the left. Interestingly, since these leakage chirps are separated and have different chirp rates, it may be possible to suppress them via the use of time-frequency analysis techniques.

5. SUMMARY AND CONCLUSIONS

Tissue harmonic imaging takes advantage of the nonlinear distortion of ultrasound waves in tissue and the associated generation of higher harmonics to obtain images with potentially improved clarity. However, since the generated higher harmonics are generally weaker than the fundamental signal, it may be useful to use techniques like coded excitation to increase SNR and improve signal penetration. Between the two useful types of codes in ultrasound, namely binary codes and FM chirps, FM signals are more readily applicable to tissue harmonic imaging as the harmonics still retain their coded phase relationship.

In this paper, the potential of linear FM chirps as codes in tissue harmonic imaging was examined. Specifically, we have studied the effects of bandwidth and pulse shaping on the compressed harmonic signals. The study was carried out through simulation means by using a step-wise nonlinear simulator that can compute the pressure field corresponding to the transmission of FM chirps (f_o=2 MHz, p_o=500 kPa) from a 1cm-radius focused disc transducer into a homogenous, tissue-mimicking material. The focal point signals were compressed using a filter that is matched to the square of the transmitted signal. The compressed harmonic signals were then analyzed based on several criteria, including mainlobe width, sidelobe levels, and SNR gain relative to a non-coded pulse. Our simulations indicate that even though coding potentially increases the SNR, the compression process can result in creation of high-magnitude sidelobes. Since these sidelobes increase with FM chirping bandwidth and can theoretically be eliminated using pulse inversion, it was concluded that they are attributed to spectral overlap of the adjacent harmonics. To reduce the sidelobe magnitudes, the leaking fundamental and third harmonic bands must be removed prior to computing the compressed harmonic signal. However, since these leaking frequency bands are not separable in the frequency domain, they cannot be removed effectively using conventional bandpass filtering. Alternatively, it may be possible to take advantage of the properties of FM chirps in the joint time-frequency domain where the various harmonics of a chirp are separable.

ACKNOWLEDGEMENTS

We are grateful for the help from Aziza Manceur on the French translations of our abstract. We also wish to thank Derek Wright for assisting us with some of the figures.

This work was supported in part by grants from the Canadian Institutes of Health Research and the Natural Sciences and Engineering Research Council of Canada.

REFERENCES

[1] RSC Cobbold, *Foundations of Biomedical Ultrasound*. New York City, USA: Oxford University Press, 2006.

[2] S Ohtsuki and M Okujima, "Ultrasonic Doppler velocity meter by M-sequence modultaion method" (in Japanese), *J. Acoust. Soc. Japan*, vol. 29, pp. 347-355, 1973. [See also: the conference presentation listings of 1970 in [3].]

[3] Y Takeuchi, "An investigation of a spread energy method for medical ultrasound systems. Part one: theory and investigation", *Ultrasonics*, vol. 17, pp. 175-182, 1979.

[4] Y Takeuchi, "An investigation of a spread energy method for medical ultrasound systems. Part two: proposed system and possible problems", *Ultrasonics*, vol. 17, pp. 219-224, 1979.

[5] M O'Donnell, "Coded excitation system for improving the penetration of real-time phased-array imaging systems", *IEEE Trans. Ultrason. Ferroelect. Freq. Contr.*, vol. 39, pp. 341-351, 1992.

[6] PM Woodward, *Probability and Information Theory, with Applications to Radar*. London, UK: Pergamon Press, 1953.

[7] CE Cook and M Bernfeld, *Radar Signals: An Introduction to Theory and Application*. New York City, USA: Academic Press, 1967 (republished: Artech House Inc., Boston, 1993).

[8] MA Benkhelifa, M Gindre, JY Le Huerou, and W Urbach, "Echography using correlation techniques: choice of coding signal", *IEEE Trans. Ultrason. Ferroelect. Freq. Contr.*, vol. 41, pp. 579-587, 1994.

[9] T Misaridis and JA Jensen, "Use of modulated excitation signals in medical ultrasound. Part I: Basic concepts and expected benefits", *IEEE Trans. Ultrason. Ferroelect. Freq. Contr.*, vol. 52, pp. 177-191, 2005.

[10] T Misaridis and JA Jensen, "Use of modulated excitation signals in medical ultrasound. Part II: Design and performance for medical imaging applications", *IEEE Trans. Ultrason. Ferroelect. Freq. Contr.*, vol. 52, pp. 192-207, 2005.

[11] DH Simpson, CT Chin, and PN Burns, "Pulse inversion Doppler: a new method for detecting nonlinear echoes from microbubble contrast agents", *IEEE Trans. Ultrason. Ferroelect. Freq. Contr.*, vol. 46, pp. 372-382, 1999.

[12] M Kowatsch and HR Stocker, "Effect of Fresnel ripples on sidelobe suppression in low time-bandwidth product linear FM pulse compression", *IEE Proc. Part-F*, vol. 129, pp. 41-44, 1982.

[13] M Pollakowski, H Ermert, L von Bernus, and T Schmeidl, "The optimum bandwidth of chirp signals in ultrasonic applications", *Ultrasonics*, vol. 31, pp. 417-420, 1993.

[14] RY Chiao and X Hao, "Coded excitation for diagnostic ultrasound: a system developer's perspective", *IEEE Trans. Ultrason. Ferroelect. Freq. Contr.*,vol.52, pp.160-170, 2005.

[15] PC Li, "Pulse compression for finite amplitude distortion based harmonic imaging using coded waveforms", *Ultrason. Imaging*, vol. 21, pp. 1-16, 1999.

[16] DY Kim, JC Lee, SJ Kwon, and TK Song, "Ultrasound second harmonic imaging with a weighted chirp signal", *Proc. IEEE Ultrason. Symp.*, pp. 1477-1480, 2001.

[17] CC Shen and PC Li, "Motion artifacts of pulse inversion-based tissue harmonic imaging", *IEEE Trans. Ultrason. Ferroelect. Freq. Contr.*, vol. 49, pp. 1203-1211, 2002.

[18] RJ Zemp, J Tavakkoli, and RSC Cobbold, "Modeling of nonlinear ultrasound propagation in tissue from array transducers", *J. Acoust. Soc. Am.*, vol. 113, pp. 139-152, 2003.

[19] PT Christopher and KJ Parker, "New approaches to nonlinear diffractive field propagation", *J. Acoust. Soc. Am.*, vol. 90, pp. 488-499, 1991.

[20] P Phukpattaranont and ES Ebbini, "Post-beamforming second-order Volterra filter for pulse-echo ultrasonic imaging", *IEEE Trans. Ultrason. Ferroelect. Freq. Contr.*, vol. 50, pp. 987-1001, 2003.